Chemical Physics Impact 7 (2023) 100318

Contents lists available at ScienceDirect

Chemical Physics Impact

journal homepage: www.sciencedirect.com/journal/chemical-physics-impact

A facile detection of ethanol by the Be/Mg/Ca-enhanced fullerenes: Insights from density functional theory

F. Toiserkani [a], M. Mirzaei [b], V. Alcan [c], K. Harismah [d,*], M.M. Salem-Bekhit [e]

[a] School of Polymer Science and Polymer Engineering, The University of Akron, Akron, OH 44325, United States
[b] Laboratory of Molecular Computations (LMC), Department of Natural and Mathematical Sciences, Faculty of Engineering, Tarsus University, Tarsus, Turkey
[c] Department of Electrical and Electronics Engineering, Faculty of Engineering, Tarsus University, Tarsus, Turkey
[d] Department of Chemical Engineering, Faculty of Engineering, Universitas Muhammadiyah Surakarta, Surakarta, Indonesia
[e] Department of Pharmaceutics, College of Pharmacy, King Saud University, Riyadh 11451, Saudi Arabia

ARTICLE INFO

Keywords:
Adsorption
Alcohol
Dopant
Fullerene
Interaction
Sensor

ABSTRACT

This work was done due to a need of developing a facile detection platform of ethanol (EtOH) type of alcohol for various reasons from the police uses up to the medical and industrial uses. To this aim, a representative model of fullerene (FULL) was doped by each of the beryllium (Be), magnesium (Mg), and calcium (Ca) alkali-earth atoms to produce MFULL counterparts including BeFULL, MgFULL, and CaFULL to be examined towards the adsorption of EtOH substance. Accordingly, the models were stabilized and their structural features were evaluated in addition to the evaluation of electronic based frontier molecular orbital features. The results showed possibility of formation of EtOH@FULL and EtOH@MFULL complexes by a priority of formation of the doped models, in which the formation of EtOH@BeFULL complex was found at the highest level of suitability regarding the energy terms and integration details. Subsequently, the electronic features indicated measurable variation of molecular orbital levels to approach a point of detection of adsorbed EtOH by the assistance of fullerenes. Meaningful results were found by performing density functional theory (DFT) calculations for showing the stability of EtOH@MFULL complexes besides evaluating measurable electronic features. Accordingly, the idea of developing a facile detection of EtOH by the Be/Mg/Ca-enhanced fullerenes was affirmed.

Introduction

Ethanol (EtOH); ethyl alcohol, grain alcohol, drinking alcohol, or just "alcohol", with the formula C_2H_5OH, is a very well-known organic chemical compound not only for the experts but also for the whole people [1]. EtOH, which is a colorless, volatile, and flammable liquid, has many important functions in producing so many types of drugs and alcoholic drinks besides its industrial roles as a chemical reagent, a solvent, and a fuel resource [2–5]. EtOH could be produced by both of natural and synthetic ways, in which its storage and further applications are among the most critical issues about dealing with EtOH [6]. In the case of very common consumption of alcoholic drinks, it should be avoided to drink it immediately with other drugs and also before driving [7]. As overdose of EtOH could also lead to serious poisoning to the human biology system [8]. In this case, providing a facile detection platform towards the existence of EtOH could help the recognition of such an overdose consumption or even chelating the extra concentration of alcohol to reduce the negative impacts [9]. To this aim, several efforts have been done to this time to explore novel detectors towards the existence of EtOH especially for recognition purposes and employing further actions [10]. It is known that the consumption of EtOH is very dangerous for driving a car because of lowering the awareness, in which one of the most important applications of EtOH detectors is their use by traffic police officers to check the status of drivers [11]. Hence, preparing a facile platform could be helpful with different aspects of dealing with EtOH in all of scientific, industrial, and general areas [12]. Among the earlier efforts, the nanostructures have been found as suitable adsorbent materials because of their high area surface feature for involving in interactions with other substances [13–15]. Both of covalent and non-covalent interactions could be considered for the case of EtOH detection for working gas a removal agent or only a sensor device [16]. Accordingly, learning details of interactions between the adsorbent and EtOH could help to investigate a customized platform for pushing forward the purpose of developing a facile detection [17].

* Corresponding author.
E-mail address: kun.harismah@ums.ac.id (K. Harismah).

https://doi.org/10.1016/j.chphi.2023.100318
Received 7 September 2023; Received in revised form 20 September 2023; Accepted 20 September 2023
Available online 21 September 2023
2667-0224/© 2023 The Authors. Published by Elsevier B.V. This is an open access article under the CC BY license (http://creativecommons.org/licenses/by/4.0/).

Besides, the nature of interactions could be also important to provide a chelator or just a sensor for the case of EtOH detection.

The characteristic features of nanostructures have been mainly dependent on their high area surface, in which distinguished them form all other related materials [18–20]. By the innovation of carbon nanotubes, several other types of nanostructures and their features were characterized for working in different purposes and processes [21–24]. Involving in adsorption functions, was indeed one of the main expectations from the newly known materials [25–27]. To this aim, several types of nanostructures were recognized for successfully approaching such an important adsorption purpose [28–30]. Among the available and known nanostructures, fullerenes have been found as very useful substances for providing both of high are surface and a single-standing molecular system avoiding the impacts of planar or tubular edges conditions [31–35]. Earlier efforts also indicated that the original fullerenes or atomic-enhanced structures could work as possible adsorbents towards the external substances [36–40]. Indeed, the atomic-enhancement was seen to be a suitable way to improve the features of nanostructures especially regarding the semi-conductivity features for approaching more appropriate sensing functions [41–45]. Accordingly, the fullerene of this work was enhanced by inserting each of beryllium (Be), magnesium (Mg), and calcium (Ca) atoms in the content of original carbon fullerene to bring a metallofullerene (MFULL) species (Fig. 1) for working as a possible adsorbent towards the EtOH substance. The alkali-earth atoms are very famous for their reactivity, and it could be supposed that employing such enhancement could lead to a more reactive metallofullerene for approaching a facile detection platform. To this aim, possible interaction configurations between EtOH and each of enhanced metallofullerene were investigated to obtain the optimized EtOH@MFULL compounds for assessing the formation of bimolecular complex models (Fig. 2). Quantum chemical based density functional theory (DFT) calculations were performed to optimize the geometries of single EtOH and MFULL structures and also their EtOH@MFULL bimolecular combinations. In this regard, both of structural and electronic features were evaluated (Figs. 1–3 and Tables 1 and 2) to learn formations details of such complexes to propose them for a possible facile detection platform towards the multi-function EtOH substance.

Materials and methods

A representative model of carbon fullerene (C_{20}) was investigated in this work as the reference structure (FULL), in which one atom was substituted by each of Be, Mg, and Ca atoms to produce enhanced MFULL substance (Fig. 1). BeFULL, MgFULL, and CaFULL were constructed by the formulas $C_{19}Be$, $C_{19}Mg$, and $C_{19}Ca$, by substituting one M atom instead of one carbon atom in the models. Optimization calculations were performed to obtain the stabilized structures for involving the bimolecular models in the interacting systems. Next, the bimolecular optimization calculations yielded the complexes in Fig. 2 including EtOH@FULL, EtOH@BeFULL, EtOH@MgFULL, and EtOH@CaFULL complexes. In this case, the stabilized geometries and energies were calculated in the current step of calculations. Interactions details were evaluated using the quantum theory of atoms in molecules (QTAIM) analyses for recognizing both of types and strengths of involving interactions in the complexes. The structural and energetic features were summarized in Table 1. To characterize the electronic features, energy levels of frontier molecular orbitals including the highest occupied and

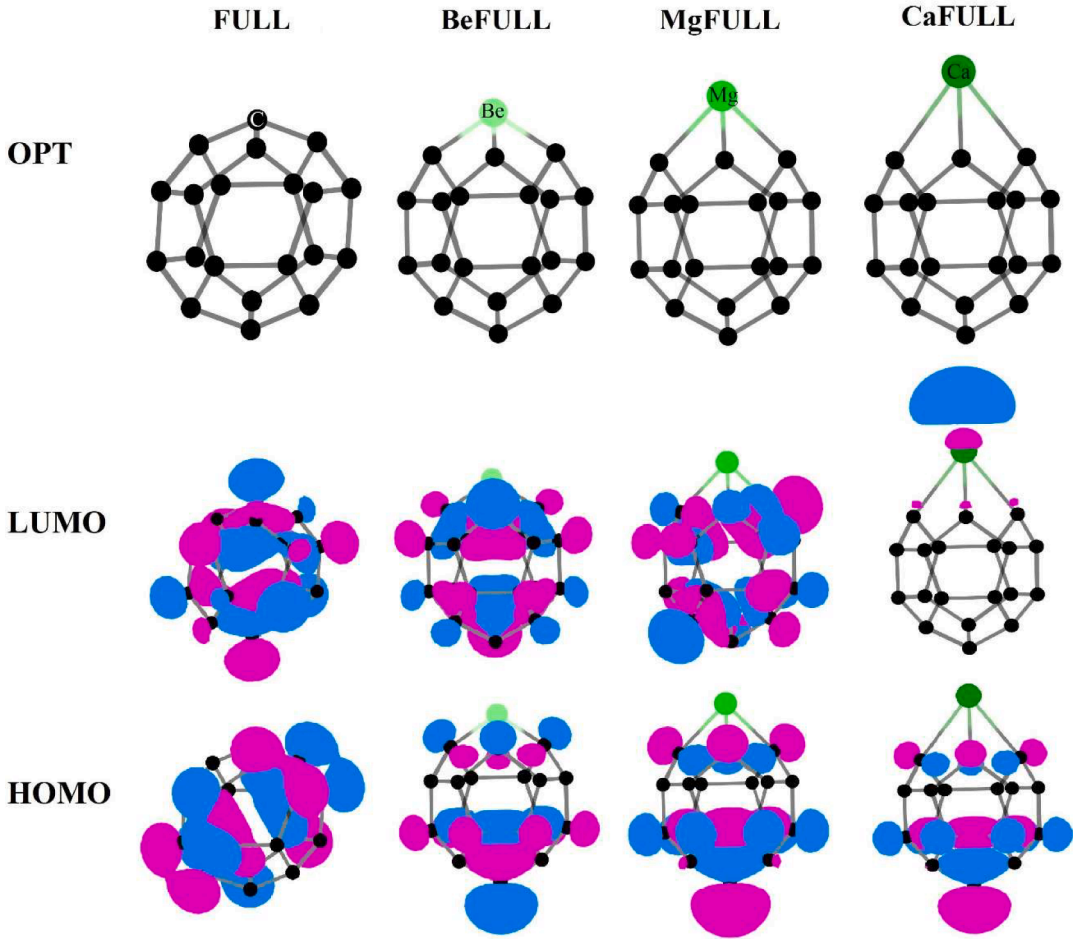


Fig. 1. Optimized models of singular fullerenes and HOMO-LUMO distribution patterns.

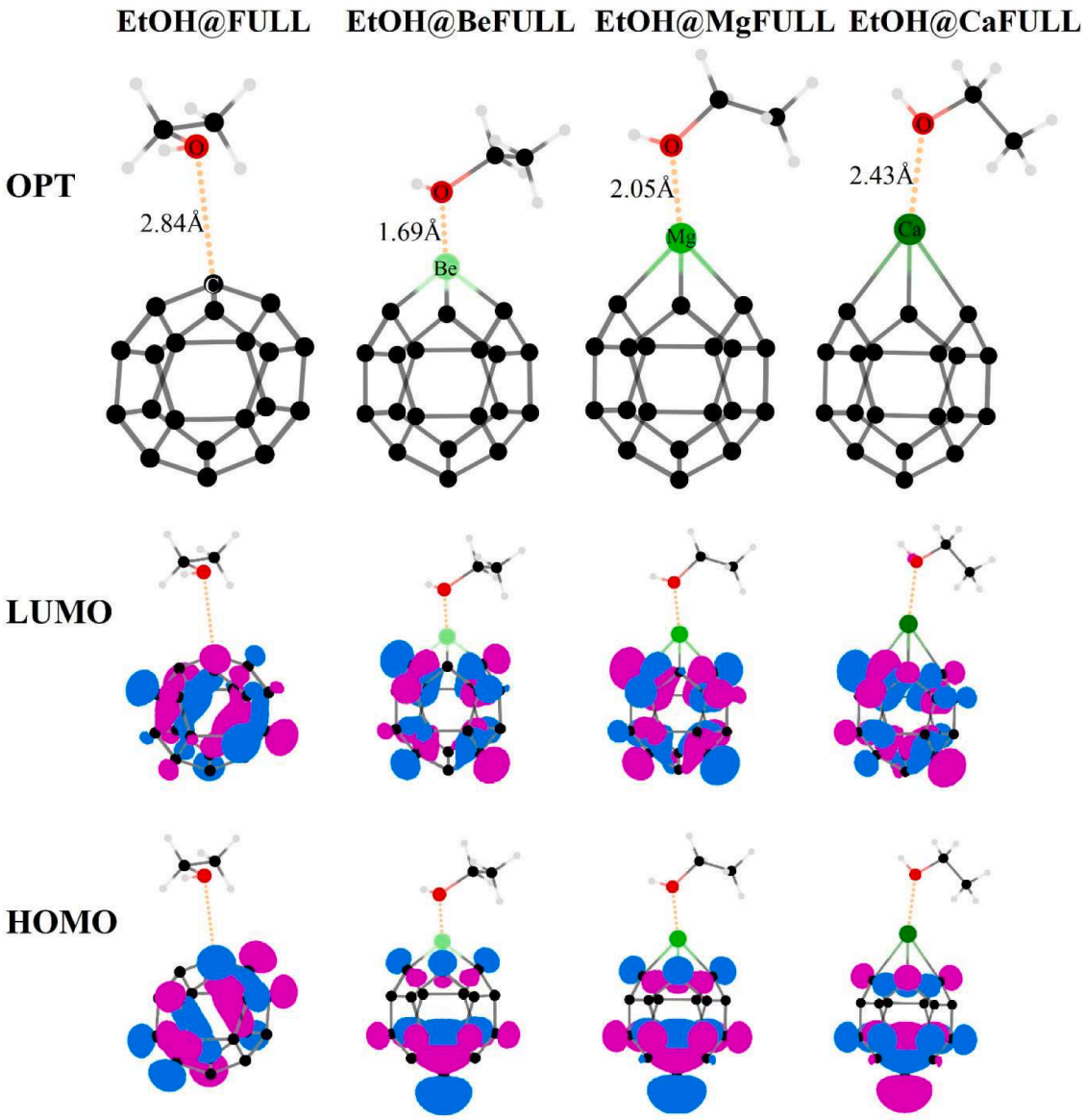


Fig. 2. Optimized models of complexes and HOMO-LUMO distribution patterns.

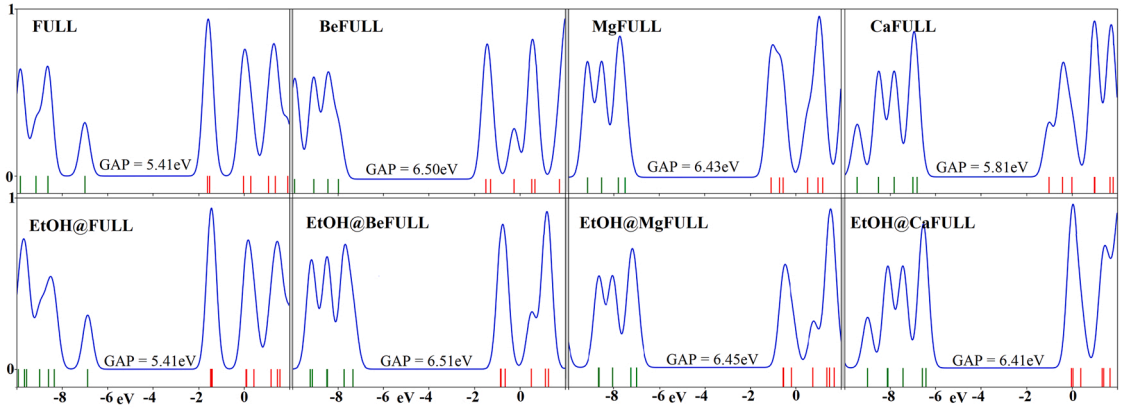


Fig. 3. DOS diagrams of optimized models of singular fullerenes and complexes.

the lowest unoccupied molecular orbitals (HOMO and LUMO) were calculated and their related features were evaluated (Table 2). Additionally, the HOMO and LUMO distribution patterns were exhibited in Figs. 1 and 2 and the diagrams of density of states (DOS) were illustrated in Fig. 3. In this regard, the models were characterized regarding their structural and electronic features to approach the goal of this work for

Table 1
Details of interacting complexes.

Feature	EtOH@FULL	EtOH@BeFULL	EtOH@MgFULL	EtOH@CaFULL
E_{Ads} kcal/mol	−2.44	−30.83	−30.50	−26.54
Interaction	O…C	O…Be	O…Mg	O…Ca
Distance Å	2.84	1.69	2.05	2.43
Rho au	0.0129	0.0563	0.0357	0.0293
Del^2-Rho au	0.0361	0.4514	0.2711	0.0148
H au	0.0004	0.0123	0.0115	0.0036

Table 2
Details of frontier molecular orbital features *.

Feature	EtOH@FULL	EtOH@BeFULL	EtOH@MgFULL	EtOH@CaFULL
LUMO eV	−1.47 [−1.60]	−0.84 [−1.49]	−0.56 [−1.08]	−0.02 [−1.01]
HOMO eV	−6.88 [−7.01]	−7.35 [−7.99]	−7.01 [−7.51]	−6.43 [−6.82]
GAP eV	6.41 [5.41]	6.45 [6.50]	6.51 [6.43]	5.41 [5.81]
%ΔGAP	0.02	0.14	0.32	10.49
CP eV	−4.17 [−4.30]	−4.09 [−4.74]	−3.78 [−4.24]	−3.23 [−3.91]
CH eV	2.70 [2.70]	3.25 [3.25]	3.22 [3.21]	3.21 [2.90]

* The values of singular fullerenes are listed in the brackets.

exploring a facile detection of EtOH by the MFULL along with DFT insights. The wB97XD/6–31+*G** level of DFT calculations were performed using the Gaussian program [46]. Indeed, the current work was done by the benefits of employing computational chemistry tools to produce reliable results for investigating the chemical systems [47–50]. Accordingly, the quantitative results of this work were summarized in Tables 1 and 2 and graphical representations were exhibited in Figs. 1–3 including the optimized models and their evaluated features.

Results and discussion

An idea of proposing an enhanced fullerene sensor material for managing a facile detection of ethanol (EtOH) was assessed within this work by performing DFT calculations. The investigated sensor models were based on the decoration of a pure carbon fullerene (FULL) by one of beryllium (Be), magnesium (Mg), and calcium (Ca) atoms to produce BeFULL, MgFULL, and CaFULL structures (Fig. 1). All three MFULL models and the referenced FULL model were optimized to reach their minimized energy geometrical structures to be prepared for participating in interactions with the EtOH substance. To this aim, combinations of EtOH substance with each of FULL, BeFULL, MgFULL, and CaFULL counterparts were explored, in which one optimum bimolecular configuration was found for each interacting system. As shown in Fig. 2, the bimolecular models were including EtOH@FULL, EtOH@BeFULL, EtOH@MgFULL, and EtOHCa@FULL complexes as indicated by their interaction between the O atomic site of EtOH and the C and M atoms of FULL and MFULL counterparts. The achievements of complex formations were affirmed by performing additional QTAIM analyses indicating details of interacting complexes through the parameters such as interaction type, distance, density of all electrons (Rho), Laplacian of electron density (Del^2-Rho), and energy density (H) [51,52]; as listed in Table 1. In addition to these features, the structural energies were calculated and summarized into the adsorption energy (E_{Ads}) values to learn the total strength of adsorption of EtOH substance by each of the FULL and MFULL counterparts. To do this, the basis set superposition error (BSSE) was also calculated not to overestimate the calculated energy values [53]. Subsequently, the evaluated energies were inserted in Eq. (1) to evaluate the EAds values for the complexes.

$$E_{Ads} = E_{Complex} - E_{EtOH} - E_{Fullerene} + BSSE \quad (1)$$

In this regard, the strengths of complexes were organized in this order EtOH@BeFULL (−30.83 kcal mol) > EtOH@MgFULL (−30.50 kcal mol) > EtOH@CaFULL (−26.54 kcal mol) > EtOH@FULL (−2.44 kcal mol) showing the highest strength for the EtOH@BeFULL complex towards the weakest EtOH@FULL complex. Herein, the initial idea of fullerene enhancement was affirmed by such achievement of a higher adsorption energy for the MFULL substances in comparison with the original FULL substance. Indeed, the formation of O…M interactions was found very better than the formation of O…C interaction, in which the results of QTAIM features indicated details of such systems regarding the electronic based values of interactions. It should be mentioned that the models were found mainly by the existence of non-covalent interactions between the counterparts, in which the interactions were still strong for keeping the counterparts to each other. Additionally, the energy features affirmed the formation of complex states but with different strengths for different complex systems.

With the evaluated distance of O…C and O…M interactions, the O…C interaction (2.84 Å) was located at the longest distance whereas the O…Be interaction (1.69 Å) was located at the shortest distance for positioning the EtOH and fullerenes towards each other. The distances for other complexes were found to be 2.05 Å for the O…Mg interaction and 2.43 Å for the O…Ca interaction in the EtOH@MgFULL and EtOH@CaFULL complexes. Analyzing the evaluated values of Rho, Del^2-Rho, and H for the complexes showed highest portion of electronic features for the EtOH@BeFULL complex in contrast with the lowest portion of electronic features for the EtOH@FULL complex. The values of EtOH@MgFULL and EtOH@CaFULL were ordered in the middle states regarding their strengths orders. As a consequence of this part, the models of EtOH@FULL and EtOH@MFULL complexes were stabilized and their features indicated an advantage of enhancement of MFULL substances for obtaining a better strength of interactions in comparison with the original FULL substance with the highest significance for the BeFULL substance for the formation of EtOH@BeFULL complex. It is worth to mention that the complex models were stabilized and their total energies were evaluated, in which the QTAIM based details (Table 1) indicated the interactions and their features inside the complex systems by a significant role of doped region for managing the interactions of complexes.

Besides obtaining the structural features and stabilities for the investigating models; as discussed above, the frontier molecular orbital features were also evaluated to show electronic specifications. The HOMO and LUMO distribution patterns were exhibited in Figs. 1 and 2, t, in which the impact of atomic doped region was found significant for the localization the main frontier molecular orbitals in the singular models. In this regard, the models were found suitable for participating in interactions with the EtOH substance through the doped region. Subsequently, the distribution patterns of complexes indicated a significant role of fullerenes for successfully adsorbing the EtOH substance through the formation of EtOH@FULL and EtOH@MFULL complexes, in which the patterns were all localized at the site of fullerene counterpart keeping the EtOH site free of any localization. This achievement is very important because of the adsorbent role of fullerene to show the significance of keeping the adsorbate at the fullerene site for yielding a managing role of interactions. In this case, the electronic features of complex models were actually defined by the significant role of fullerene counterpart. To more explain such achievements, the variations of

molecular orbitals around the frontier molecular orbitals were also determined by the illustrated DOS diagrams Fig. 3), which showed a measurable variations for the investigated systems. The energy gap distance of HOMO and LUMO levels was defined by the GAP value (Eq. (2)), and the variation of GAP from a singular fullerene to its corresponding complex was defined by the%ΔGAP value (Eq. (3)), which were all discussable for the models of this work [54]. Additional related features including the chemical potential (CP) and chemical hardness (CH) were also evaluated using Eqs. (4) and ((5) and all the frontier molecular orbital quantities were summarized in Table 2. Based on the obtained properties, the electronic features of investigated models could be recognized based on their existences in different states and systems, in which following the variations could help to approach the sensing functions.

$$GAP = LUMO - HOMO \tag{2}$$

$$\%\Delta GAP = 100 \times \left\{ \left(GAP_{Complex} - GAP_{Fullerene} \right) / GAP_{Fullerene} \right\} \tag{3}$$

$$CP = 1/2(LUMO + HOMO) \tag{4}$$

$$CH = 1/2(LUMO - HOMO) \tag{5}$$

From a singular fullerene to its corresponding complex, the variations of exact levels of HOMO and LUMO were found very significant; however, the GAP values were almost similar with the exception of the singular CaFULL conversion to the EtOH@CaFULL complex. By the %Δ GAP values, it could be found that the measurement of only the GAP changes might not be enough for recognizing such complicated systems, but examining the variations of exact levels of HOMO and LUMO and their surrounding molecular orbitals could be considered as a better tool. In this regard, measuring the variations of molecular orbitals along with the DOS diagrams could be even more useful for approaching a meaningful result about the mechanism of detection and adsorption of EtOH by the fullerene adsorbents. On the other hand, comparing the values of CP and CH of singular and complex models indicated an electronic stability for the models regarding their further usage for sensing purposes. This achievement could mean that the fullerene models were still re-usable regarding their electronic features stability.

Returning again to the features of stabilities and frontier molecular orbitals, the terms of “recovery time” and “conductance rate” could be followed by the calculated values of E_{Ads} and %ΔGAP, in which the longest recovery time could be supposed for the strongest EtOH@BeFULL complex and the highest conductance rate changes could be found for the EtOH@CaFULL complex. It is worth to mention that the evaluated results indicated benefits of employing the atomic doped FULL counterparts instead of the original FULL for adsorbing the EtOH substance in a more facile way. However, various features were still found among the doped fullerenes showing their structural and electronic variations due to the type of doping atom. Hence, it could be learned that the customization of a nanostructures for working in a specific purpose is indeed a multi-task activity depending on several structural and electronic features, which should be know prior to their using.

Conclusions

The main idea of this work for developing a facile detection platform of EtOH was followed by assessing each of FULL, BeFULL, MgFULL, and CaFULL counterparts along with DFT calculations. The achieved results were divided into some notes. First, the models were stabilized by toe formation of interaction between the EtOH and fullerene substances. Second, the strengths of complexes were different, in which the formations of EtOH@MFULL complexes were more suitable than the formation of EtOH@FULL complex showing the importance of atomic doping of fullerene for approaching a better results of complex strength. Third, the formation of EtOH@BeFULL complex was found as the most suitable one regarding the interaction strength among the obtained models. Fourth, the frontier molecular orbital features indicated variation of exact levels of HOMO and LUMO in all the models with a more significant of such variations for the singular CaFULL conversion to the EtOH@CaFULL complex. Fifth, the facile detection of EtOH could be achieved by the assistance of each of MFULL substances with a priority of recovery time for the EtOH@BeFULL complex and a priority of conductance rate change for the EtOH@CaFULL complex. As a final remark, a need to manage a facile detection of EtOH could be resolved by the assistance of MFULL substances for various purposes of sensing and removal processes.

CRediT authorship contribution statement

F. Toiserkani: Formal analysis, Investigation, Writing – original draft. **M. Mirzaei:** Investigation, Methodology, Writing – original draft. **V. Alcan:** Software, Visualization, Validation, Writing – review & editing. **K. Harismah:** Conceptualization, Supervision, Validation, Writing – review & editing. **M.M. Salem-Bekhit:** Conceptualization, Funding acquisition, Writing – review & editing.

Declaration of Competing Interest

The authors declare that they have no known competing financial interests or personal relationships that could have appeared to influence the work reported in this paper.

Acknowledgments

The authors would like to extend their sincere appreciation to the Researchers Supporting Project Number (RSPD2023R986), King Saud University, Riyadh, Saudi Arabia.

References

[1] A. Vale, Ethanol, Medicine 35 (2007) 615 (Baltimore).
[2] A.Z. Mendiburu, C.H. Lauermann, T.C. Hayashi, D.J. Mariños, R.B. da Costa, C. J. Coronado, J.J. Roberts, J.A. de Carvalho Jr, Ethanol as a renewable biofuel: combustion characteristics and application in engines, Energy 257 (2022), 124688.
[3] R. Yuliani, F. Syahdeni, Ethanolic extract of papaya leaves (Carica papaya) and its fractions have no potential cytotoxicity on T47D cells, Pharm. J. Farm. Indones. 17 (2020) 17.
[4] P. Indrayudha, Antibacterial activity of combination of ethanol extract of pepermine leaves (mentha piperita L.) and amikacin against klebsiella pneumonia, staphylococcus aureus, and escherichia coli, J. Nutraceuticals Herb. Med. 4 (2021) 12.
[5] F. Karimah, A. Sa’adi, W. Widjiati, The ethanolic extract of basic leaves (Ocimum basilicum) effect on expression of follicle stimulating hormone receptors (FSHr) and folliculogenesis in female mice model endometriosis, J. Med. Chem. Sci. 6 (2023) 2896.
[6] C.C. Geddes, I.U. Nieves, L.O Ingram, Advances in ethanol production, Curr. Opin. Biotechnol. 22 (2011) 312.
[7] A.W. Jones, Driving under the influence of alcohol, Handb. Forensic Med. 3 (2022) 1387.
[8] L.A. Lin, E.E. Bonar, L. Zhang, R. Girard, L.N. Coughlin, Alcohol-involved overdose deaths in US veterans, Drug Alcohol Depend. 230 (2022), 109196.
[9] H.Y. Peng, W. Wang, F.H. Gao, S. Lin, X.J. Ju, R. Xie, Z. Liu, Y. Faraj, L.Y. Chu, Smart hydrogel gratings for sensitive, facile, and rapid detection of ethanol concentration, Ind. Eng. Chem. Res. 58 (2019) 17833.
[10] L.Y. Gai, R.P. Lai, X.H. Dong, X. Wu, Q.T. Luan, J. Wang, H.F. Lin, W.H. Ding, G. L. Wu, W.F. Xie, Recent advances in ethanol gas sensors based on metal oxide semiconductor heterojunctions, Rare Met. 41 (2022) 1818.
[11] B.K. Singh, Forensic perspective of detecting ethanol with a breath analyser, Med. Leg. J. 91 (2023) 42.
[12] M. Asgari, F.H. Saboor, S.P. Amouzesh, M.W. Coull, A.A. Khodadadi, Y. Mortazavi, T. Hyodo, Y. Shimizu, Facile ultrasonic-assisted synthesis of SiO2/ZnO core/shell nanostructures: a selective ethanol sensor at low temperatures with enhanced recovery, Sens. Actuators B Chem. 368 (2022), 132187.
[13] K.G. Krishna, S. Parne, N. Pothukanuri, V. Kathirvelu, S. Gandi, D. Joshi, Nanostructured metal oxide semiconductor-based gas sensors: a comprehensive review, Sens. Actuators A Phys. 341 (2022), 113578.
[14] K. Harismah, M. Mirzaei, Complex formations of favipiravir and BeO-decorated carbon nanocones along with quantum processing, Biointerface Res. Appl. Chem. 13 (2023) 508.
[15] R.D. Pecho, N. Hajali, R.D. Tapia-Silguera, L. Yassen, M. Alwan, M.J. Jawad, F. Castro-Cayllahua, M. Mirzaei, Akhavan-Sigari R. Molecular insights into the

sensing function of an oxidized graphene flake for the adsorption of avigan antiviral drug, Comput. Theor. Chem. 1227 (2023), 114240.
[16] E. Lim, X. Hong, M.K. Tan, H. Yu, H. Wu, Y.M. Hung, Distinctive evaporation characteristics of water and ethanol on graphene nanostructured surfaces, Int. J. Heat Mass Transf. 183 (2022), 122174.
[17] M. Aleksanyan, A. Sayunts, G. Shahkhatuni, Z. Simonyan, G. Shahnazaryan, V. Aroutiounian, Gas sensor based on ZnO nanostructured film for the detection of ethanol vapor, Chemosensors 10 (2022) 245.
[18] M.N. Awan, H. Razzaq, O.U. Abid, S. Qaisar, Recent advances in electroanalysis of hydrazine by conducting polymers nanocomposites: a review, J. Chem. Rev. 5 (2023) 311.
[19] Y. Masuda, Recent advances in SnO2 nanostructure based gas sensors, Sens. Actuators B Chem. 364 (2022), 131876.
[20] W.S. Choi, H.J. Lee, Nanostructured materials for water purification: adsorption of heavy metal ions and organic dyes, Polymers 14 (2022) 2183 (Basel).
[21] M. Manuel, A Jennifer, A review on starch and cellulose-enhanced superabsorbent hydrogel, J. Chem. Rev. 5 (2023) 183.
[22] R. Shete, P. Fernandes, B. Borhade, A. Pawar, M. Sonawane, N. Warude, Review of cobalt oxide nanoparticles: green synthesis, biomedical applications, and toxicity studies, J. Chem. Rev. 4 (2022) 331.
[23] R. Khazaei, A. Khazaei, M. Nasrollahzadeh, Horsetail assisted green synthesis of Fe3O4@SiO2-Pd: a reusable and highly efficient magnetically separable catalyst for suzuki coupling reactions, J. Appl. Organomet. Chem. 3 (2023) 123.
[24] F. Banifatemeh, Polymerization of graphite and carbon compounds by aldol condensation as anti-corrosion coating, Asian J. Green Chem. 7 (2023) 25.
[25] A. Heidaripour, F. Salmani, T. Barati, Synthesis of coral-like ZnO nanostructures with high and wide absorption range, Asian J. Green Chem. 7 (2023) 140.
[26] S.M. Abegunde, K.S. Idowu, Enhanced adsorption of methylene blue dye from water by alkali-treated activated carbon, Eurasian J. Sci. Technol. 3 (2023) 109.
[27] N. Farhami, A computational study of thiophene adsorption on boron nitride nanotube, J. Appl. Organomet. Chem. 2 (2022) 148.
[28] F. Ahmad, K. Kainat, U. Farooq, A comprehensive review on materials having high oxygen reduction reaction (ORR) activity, J. Chem. Rev. 4 (2022) 374.
[29] B. Baghernejad, M. Alikhani, Nano-cerium oxide/aluminum oxide as an efficient catalyst for the synthesis of xanthene derivatives as potential antiviral and anti-inflammatory agents, J. Appl. Organomet. Chem. 2 (2022) 140.
[30] V. Safari Fard, Y. Davoudabadi Farahani, An amine/imine functionalized microporous MOF as a new fluorescent probe exhibiting selective sensing of Fe3+ and Al3+ Over mixed metal ions, J. Appl. Organomet. Chem. 2 (2022) 165.
[31] A.V. Baskar, M.R. Benzigar, S.N. Talapaneni, G. Singh, A.S. Karakoti, J. Yi, A.A. Al-Muhtaseb, K. Ariga, P.M. Ajayan, A. Vinu, Self-assembled fullerene nanostructures: synthesis and applications, Adv. Funct. Mater. 32 (2022), 2106924.
[32] E. Golipour-Chobar, F. Salimi, G. Ebrahimzadeh-Rajaei, Sensing of lomustine drug by pure and doped C48 nanoclusters: DFT calculations, Chem. Methodol. 6 (2022) 790.
[33] H. Darougari, M. Rezaei-Sameti, The drug delivery appraisal of Cu and Ni decorated B12N12 nanocage for an 8-hydroxyquinoline drug: a DFT and TD-DFT computational study, Asian J. Nanosci. Mater. 5 (2022) 196.
[34] M. Da'i, M. Mirzaei, F. Toiserkani, S.M. Mohealdeen, Y. Yasin, M.M. Bekhit, R Akhavan-Sigari, Sensing the formaldehyde pollutant by an enhanced BNC18 fullerene: DFT outlook, Chem. Phys. Impact 7 (2023), 100306.
[35] M. Da'i, E.R. Wikantyasning, Maryati, A.S. Wahyuni, M Mirzaei, A titanium-enhanced boron nitride fullerene for the drug delivery of 5-fluorouracil anticancer: DFT study, Biointerface Res. Appl. Chem. 13 (2023) 434.
[36] J.S. Al-Otaibi, Y.S. Mary, Y.S. Mary, Z. Ullah, R. Yadav, N. Gupta, D.G. Churchill, Adsorption properties of dacarbazine with graphene/fullerene/metal nanocages–Reactivity, spectroscopic and SERS analysis, Spectrochim. Acta A 268 (2022), 120677.
[37] B.L. Ndjopme Wandji, A.D. Tamafo Fouegue, N.K. Nkungli, R.A. Ntieche, A Wahabou, DFT investigation on the application of pure and doped X12N12 (X= B and Al) fullerene-like nano-cages toward the adsorption of temozolomide, R. Soc. Open Sci. 9 (2022), 211650.
[38] E.B. Kalika, K.P. Katin, A.I. Kochaev, S. Kaya, M. Elik, M.M. Maslov, Fluorinated carbon and boron nitride fullerenes for drug delivery: computational study of structure and adsorption, J. Mol. Liq. 353 (2022), 118773.
[39] C.G. Apebende, H. Louis, A.E. Owen, I. Benjamin, I.O. Amodu, T.E. Gber, F. C. Asogwa, Adsorption properties of metal functionalized fullerene (C59Au, C59Hf, C59Ag, and C59Ir) nanoclusters for application as a biosensor for hydroxyurea (HXU): insight from theoretical computation, Z. Phys. Chem. 236 (2022) 1515.
[40] I. Muz, Enhanced adsorption of fluoroquinolone antibiotic on the surface of the Mg-, Ca-, Fe-and Zn-doped C60 fullerenes: DFT and TD-DFT approach, Mater. Today Commun. 31 (2022), 103798.
[41] H. Louis, D.E. Charlie, I.O. Amodu, I. Benjamin, T.E. Gber, E.C. Agwamba, A. S. Adeyinka, Probing the reactions of thiourea (CH4N2S) with metals (X= Au, Hf, Hg, Ir, Os, W, Pt, and *Re*) anchored on fullerene surfaces (C59X), ACS Omega 7 (2022) 35118.
[42] S. Yeasmin, M. Mehade Hasan, A.A. Oishi, S.A. Bithe, D. Roy, A.S Rad, A first principles study of adsorption of hydrazine on C20, C40 and C60 fullerene nanoclusters, Mol. Simul. 49 (2023) 551.
[43] R. Ghiasi, F. Aghazadeh Kozeh Kanani, Theoretical insights of the electronic structures, conductivity, and aromaticiy of Graphyne and Si-doped Graphynes, Asian J. Nanosci. Mater. 5 (2022) 303.
[44] S. Noor, A. Al-Shamari, High photocatalytic performance of ZnO and ZnO/CdS nanostructures against reactive blue 4 dye, Eurasian Chem. Commun. 5 (2023) 776.
[45] M. Da'i, A.S. Wahyuni, E.R. Wikantyasning, Maryati, M. Mirzaei, Insights into the delivery of hydrea anticancer drug by the assistance of an oxidized silicon carbide nanocage, Biointerface Res. Appl. Chem. 13 (2023) 497.
[46] M.J. Frisch, G.W. Trucks, H.B. Schlegel, G.E. Scuseria, M.A. Robb, J.R. Cheeseman, et al., Gaussian 09 Program, Gaussian Inc., Wallingford, CT, 2009.
[47] N. Javadi, H. Fakhraian, Investigation of enantiomeric separation of tiletamine drug using computational chemistry methods, Eurasian Chem. Commun. 5 (2023) 661.
[48] M. Rezaei Sameti, B Amirian, A quantum, NBO, RDG study the interaction of cadmium ion with the pristine, C, P and C&P doped (4,4) armchair boron nitride nanotube (BNNTs), Asian J. Nanosci. Mater. 5 (2022) 327.
[49] K.S. Atrushi, D.M. Ameen, S.H. Abdulrahman, F.T. Abachi, Density functional theory, ADME, and molecular docking of some anthranilic acid derivatives as cyclooxygenase inhibitors, J. Med. Chem. Sci. 6 (2023) 1943.
[50] S. Ariavand, M. Ebrahimi, E. Foladi, Design and construction of a novel and an efficient potentiometric sensor for determination of sodium ion in urban water samples, Chem. Methodol. 6 (2022) 886.
[51] R.F. Bader, T.T. Nguyen-Dang, Quantum theory of atoms in molecules–Dalton revisited, Adv. Quantum Chem. 14 (1981) 63.
[52] M. Ghiasifar, T. Hosseinnejad, A. Ahangar, Copper catalyzed cycloaddition reaction of azidomethyl benzene eith 2,2-di(prop-2-yn-1-yl)propane-1,3-diol: DFT and QTAIM investigation, Prog. Chem. Biochem. Res. 5 (2022) 1.
[53] E.R. Davidson, S.J. Chakravorty, A possible definition of basis set superposition error, Chem. Phys. Lett. 217 (1994) 48.
[54] R. Rahimi, M. Solimannejad, A. Chaudhari, Toxic volatile organic compounds sensing by Al2C monolayer: a first-principles outlook, J. Hazard. Mater. 403 (2021), 123600.